論文 / 著書情報
Article / Book Information

Title	Equivalent-input-disturbance approach to active structural control for seismically excited buildings
Authors	Kou Miyamoto, Jinhua She, Junya Imani, Xin Xin, Daiki Sato
Citation	Engineering Structures, Vol. 125, pp. 392-399
Pub. date	2016, 10
DOI	http://dx.doi.org/10.1016/j.engstruct.2016.07.028
Creative Commons	See next page.
Note	This file is author (final) version.

License

Engineering Structures, Vol. 125, pp. 392–399, October 2016.
doi:10.1016/j.engstruct.2016.07.028

Equivalent-input-disturbance approach to active structural control for seismically excited buildings

Kou Miyamoto[a], Jinhua She[b,*], Junya Imani[c], Xin Xin[d], Daiki Sato[a]

[a]*School of Environment and Society, Architecture and Building Engineering, Tokyo Institute of Technology, Yokohama, Kanagawa 226-8503, Japan*
[b]*School of Engineering, Tokyo University of Technology, Hachioji, Tokyo 192-0982, Japan*
[c]*Department of Mechanical Systems Engineering, Tokyo University of Agriculture and Technology, Tokyo 184-8588, Japan*
[d]*Faculty of Computer Science and Systems Engineering, Okayama Prefectural University, Soja, Okayama 719-1197, Japan*

Abstract

A new method of active structural control, which suppresses vibrations in civil structures due to seismic shocks, has been developed. It is based on the equivalent-input-disturbance (EID) approach, which estimates the effect of a seismic shock and produces an equivalent control signal on the control input channel to compensate for it. A system designed by this method can be viewed as a conventional state-feedback control system with an EID estimator plugged in. Unlike conventional control systems, this one has two degrees of freedom, which yields better control performance. Simulations on a model of a ten-degree-of-freedom building demonstrated the validity of the method. In addition, the effect of the parameters of the low-pass filter in the EID estimator on the vibration suppression performance was examined. A comparison revealed that this method is superior to a linear-quadratic regulator and sliding-mode control.

Keywords: active structural control (ASC), equivalent input disturbance (EID), disturbance estimation, linear-quadratic regulator (LQR), sliding-mode control (SMC), seismic vibration, vibration suppression.

Nomenclature

ASC: Active structural control

DOF: Degree of freedom

EID: Equivalent input disturbance

LQR: Linear-quadratic regulator

NC: No control

PID: Proportional integral derivative

SMC: Sliding-mode control

m_i: Mass of ith DOF ($i = 1, \ldots, n$)

k_i: Stiffness of ith DOF ($i = 1, \ldots, n$)

c_i: Damping of ith DOF ($i = 1, \ldots, n$)

M_S: Mass matrix of structure

K_S: Stiffness matrix of structure

C_S: Damping matrix of structure

ω_m: Maximum angular frequency for vibration suppression

I_k: k-dimensional identity matrix

$0_{j\times k}$: j-by-k matrix with all entries being zero

$x_i(t)$: Displacement of ith DOF ($i = 1, \ldots, n$)

$\dot{x}_i(t)$: Velosity of ith DOF ($i = 1, \ldots, n$)

$\ddot{x}_i(t)$: Acceleration of ith DOF ($i = 1, \ldots, n$)

$\ddot{x}_g(t)$: Acceleration of ground

$q(t)$: Displacement vector ($= [x_1(t), x_2(t), \ldots, x_n(t)]^T$)

$\dot{q}(t)$: Speed vector ($= [\dot{x}_1(t), \dot{x}_2(t), \ldots, \dot{x}_n(t)]^T$)

$\xi(t)$: State vector ($= [q^T(t), \dot{q}^T(t)]^T$)

$\theta_i(t)$: Interstory-drift angle of ith DOF ($i = 1, \ldots, n$)

$\Delta\dot{x}_i(t)$: Relative speed of ith DOF ($i = 1, \ldots, n$)

$\ddot{x}_i(t) + \ddot{x}_g(t)$: Absolute acceleration of ith DOF ($i = 1, \ldots, n$)

$\|u\|_2$: 2-norm of signal $u(t)$, which is defined as $\|u\|_2 = \left\{\int_{-\infty}^{\infty} u^T(t)u(t)dt\right\}^{1/2}$

$\|G\|_\infty$: H_∞ norm of system $G(s)$, which is defined as $\|G\|_\infty = \sup_{0\le\omega\le\infty} \sigma_{\max}[G(j\omega)]$

$\sigma_{\max}(G)$: Maximum singular value of G

*Corresponding author. Tel. & Fax: +81-42(637)2487. *E-mail address:* she@stf.teu.ac.jp (J. She)

1. Introduction

The first full-scale implementation of active structural control (ASC) was in Kyobashi Center Building in 1989 [1]. Progress in ASC has been rapid, and it is now widely used in civil structures [2]. Since ASC pumps energy into a system to suppress vibrations, it is effective for all types of vibrations.

A variety of control strategies have been employed to design ASC systems, including the extensively used linear-quadratic regulator (LQR) [3, 4], PID control [5], computational-intelligence-based control [6, 7, 8, 9, 10, 11], predictive control [12], sliding-mode control (SMC) [13], and robust control [14, 15, 16, 17]. However, the resulting systems generally have only one degree of freedom (DOF). Note that, while the DOF is defined to be the number of modes of a building model in structural engineering, the DOF of a control system is defined to be the number of closed-loop transfer functions that can be adjusted independently in control engineering [18]. The control objective is to minimize the sensitivity function of the control system, but there are trade-offs between the sensitivity function and other aspects of control performance for a one-DOF control system.

On the other hand, She et al. devised the equivalent-input-disturbance (EID) approach, which rejects both matched and unmatched disturbances [19, 20]. An EID-based control system has two DOFs: one is used to tune the disturbance rejection performance, and the other is used to tune the feedback performance. This relaxes the trade-off between different aspects of control performance. Unlike a one-DOF system, an EID-based control system directly estimates the effect of disturbances and produces a control input that actively suppresses that effect. This makes the system more effective than a one-DOF system in suppressing vibrations due to seismic shocks, even when the same actuators are used for both systems. Some of the distinctive features of the method are that the control system has a simple structure, that it does not require the derivative of measured output, and that it avoids the cancellation of unstable poles and zeros. She et al. previously applied this method of controlling seismic vibrations to a model of a three-story building with an actuator for each story and with an input dead zone in each actuator, and presented some preliminary results in a conference paper [21].

This paper considers EID-based ASC for a seismically excited building, and examines the internal operation of the EID method for ASC. Since actuators are expensive, the fewer there are, the better. Unlike the system described in [21], the one considered in this study has fewer actuators than stories. The design of the control system is explained, and the validity of the method is demonstrated through simulations using data from five earthquakes with different kinds of seismic waves, and through a comparison with the LQR and SMC methods. The relationship between the effectiveness of vibration suppression and the input energy of the control system is examined. Most reports have shown control results only for the displacement or drift of stories. However, the velocity and acceleration of a story strongly impact the people on that floor. To better assess damage reduction and the impact on humans, this study investigated not only interstory-drift angles, but also relative velocity and absolute acceleration.

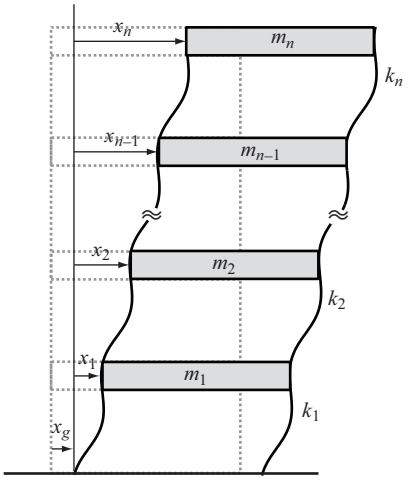

Fig. 1: n-DOF model of building.

2. Structural Model

The dynamics of an n-DOF building (Fig. 1) are described by the equation

$$M_S\ddot{q}(t) + C_S\dot{q}(t) + K_S q(t) = E_u u(t) + E_g\ddot{x}_g(t), \tag{1}$$

where

$$q(t) = [x_1(t), x_2(t), \ldots, x_n(t)]^T$$

is the displacement vector; $u(t) \in \mathbb{R}^l$ is the control force produced by an actuator; $\ddot{x}_g(t)$ is the acceleration of the ground; M_S is the mass matrix; C_S is the damping factor matrix; K_S is the stiffness matrix; and E_u and E_g are input matrices for $u(t)$ and $\ddot{x}_g(t)$, respectively.

The state-space variable, $\xi(t)$, is defined to be

$$\xi(t) = \begin{bmatrix} q(t) \\ \dot{q}(t) \end{bmatrix}, \tag{2}$$

and note that M_S is positive definite. Thus, the state-space representation of (1) is

$$\begin{cases} \dot{\xi}(t) = A\xi(t) + B_u u(t) + B_g\ddot{x}_g(t), \\ y(t) = C\xi(t), \end{cases} \tag{3}$$

where

$$A = \begin{bmatrix} 0 & I_n \\ -M_S^{-1}K_S & -M_S^{-1}C_S \end{bmatrix}, \quad B_u = \begin{bmatrix} 0 \\ M_S^{-1}E_u \end{bmatrix}, \quad B_g = \begin{bmatrix} 0 \\ M_S^{-1}E_g \end{bmatrix},$$

C is the output matrix, and $y(t) \in \mathbb{R}^p$ is the measured output of the system.

Now, we define three terms in the basic vocabulary of control engineering.

Plant: A plant is a physical object to be controlled.

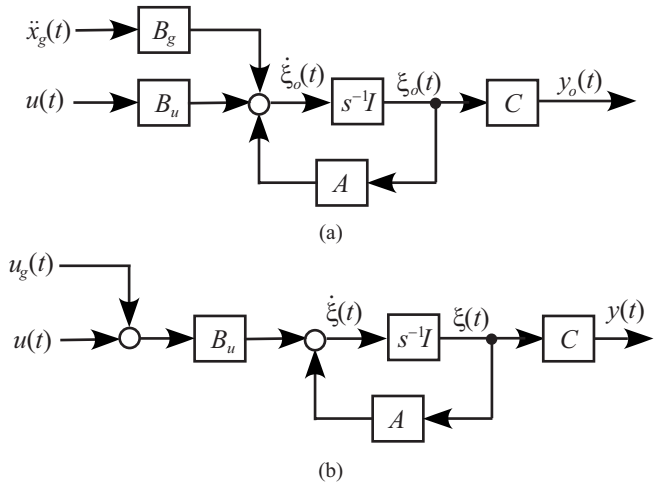

Fig. 2: Concept of EID: (a) original structural model and (b) structural model with EID.

Controllable: Controllable means that the current state of the plant can be moved by an admissible control input in the state space.

Observable: Observable means that the current state of the plant can be determined in finite time from the input and output.

For simplicity, the plant is usually described using the parameters in (3). For the plant (A, B_u, C), it is easy to verify that (A, B_u) is controllable, and (C, A) is observable. Note that (A, B_u, C) is a minimum-phase system[1] and there are no zeros on the imaginary axis. This characteristic enables us to employ the results in [19] to design an EID-based ASC system.

3. Design of EID-based ASC System

This section explains the configuration and design of an EID-based ASC system.

Figure 2 shows the original structural model and the model with an EID. As explained in [19], an EID is an input signal on the control input channel that has the same effect on the output as actual disturbances do; that is, for $u(t) = 0$ and $\xi(0) = \xi_o(0)$, if $y(t) = y_o(t)$ for all $t \geq 0$, then, $u_g(t)$ is an EID of $\ddot{x}_g(t)$. In the rest of the paper, we abused the notation a bit by using the same variables, $\xi(t)$ and $y(t)$, for both models. This should not cause confusion.

3.1. Configuration of EID-based ASC System

In the EID-based ASC system in Fig. 3,

$$B_u^+ := \left(B_u^T B_u\right)^{-1} B_u^T. \tag{4}$$

Note that B_u^+ is the pseudo-inverse of B_u and $B_u^+ = B_u^{-1}$ if B_u is an invertible square matrix.

The system has four parts:

[1] A minimum-phase system has all its poles and zeros on the complex open left-half plane.

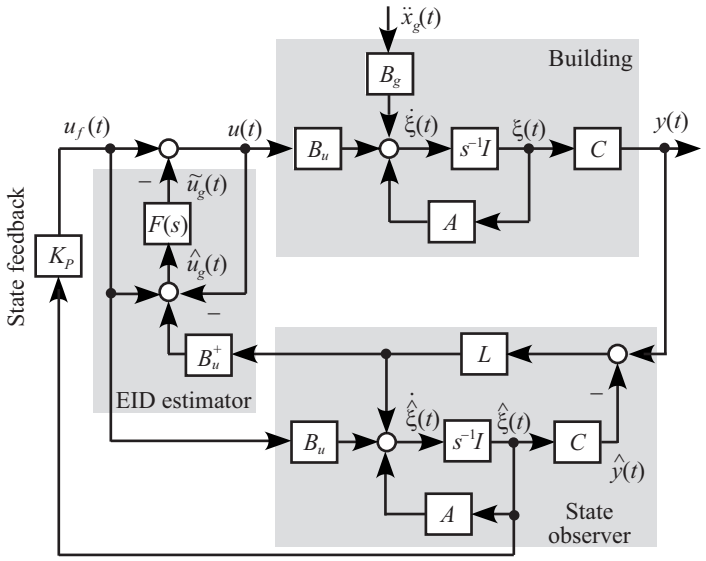

Fig. 3: Configuration of EID-based ASC system.

1) the plant, which in this study is a civil structure;
2) a state observer, which reproduces the state of the plant, $\hat{\xi}(t)$;
3) an EID estimator, which uses $\hat{\xi}(t)$ to produce an estimate of the EID; and
4) state feedback, which stabilizes the plant.

This control system can be regarded as a conventional state-feedback control system (state observer + state feedback) with an EID estimator plugged in.

The state equation of the observer is

$$\begin{cases} \dot{\hat{\xi}}(t) = A\hat{\xi}(t) + B_u u_f(t) + L\left[y(t) - \hat{y}(t)\right], \\ \hat{y}(t) = C\hat{\xi}(t). \end{cases} \tag{5}$$

The EID estimate is

$$\hat{u}_g(t) = B_u^+ LC\left[\xi(t) - \hat{\xi}(t)\right] + u_f(t) - u(t). \tag{6}$$

A low-pass filter, $F(s)$, is used to select the angular frequency band for vibration suppression. It should be designed so that

$$|F(j\omega)| \approx 1, \ \forall \omega \in [0, \omega_m], \tag{7}$$

where ω_m is the maximum angular frequency for vibration suppression. The output of the filter is

$$\tilde{U}_g(s) = F(s)\hat{U}_g(s), \tag{8}$$

where $\tilde{U}_g(s)$ and $\hat{U}_g(s)$ are the Laplace transformations of $\tilde{u}_g(t)$ and $\hat{u}_g(t)$, respectively. The modified control law

$$u(t) = u_f(t) - \tilde{u}_g(t) \tag{9}$$

combines the state-feedback control law and the filtered estimate, $\tilde{u}_g(t)$, to suppress the vibrations caused by $\ddot{x}_g(t)$.

As explained in [19], there are three stability conditions for the system:

1) $A + BK_P$ is stable.

2) $A - LC$ is stable.

3) The inequality

$$\|GF\|_\infty < 1 \tag{10}$$

holds, where

$$G(s) = B_u^+(sI - A)\left[sI - (A - LC)\right]^{-1} B_u. \tag{11}$$

It is clear from these conditions that, if the stability of the control system is the only concern, then the Separation Theorem holds; and thus the state feedback, and the observer and the low-pass filter can be designed independently.

3.2. Design of EID-based ASC System

The design parameters of the system are the state-feedback gain, K_P, the observer gain, L, and the low-pass filter in the EID estimator, $F(s)$.

As mentioned above, since the Separation Theorem holds if stability is our only concern, K_P can be designed independently of L and $F(s)$. An optimal K_P is obtained by minimizing the performance index

$$J_K = \int_0^\infty \left\{\xi^T(t)Q_K\xi(t) + u_f^T(t)R_K u_f(t)\right\} dt, \tag{12}$$

where $Q_K > 0$ and $R_K > 0$ in (12) are weighting matrices for the plant (3). It is given by

$$K_P = -R_K^{-1}B_u^T P, \tag{13}$$

where P is a positive symmetrical solution of the Riccati equation

$$A^T P + PA - PB_u R_K^{-1} B_u^T P + Q_K = 0. \tag{14}$$

Regarding the design of $F(s)$, a first-order filter,

$$F(s) = \frac{K_F}{Ts + 1} I_l, \tag{15}$$

works well, as explained in [19], where K_F is the gain of the filter. And the time constant, T, should be chosen so that

$$T \le \frac{1}{5\omega_m}. \tag{16}$$

The fact that the plant (3) is a minimum-phase system allows us to employ the design method in [19], which is based on the concept of perfect regulation, to design L. The design procedure has four steps:

Step 1. Construct a dual system of (A, B_u, C):

$$\begin{cases} \dot{\xi}_L(t) = A^T\xi_L(t) + C^T u_L(t), \\ y_L(t) = B_u^T\xi_L(t). \end{cases} \tag{17}$$

Step 2. Optimize the performance index

$$J_L = \int_0^\infty \left\{\rho\xi_L^T(t)Q_L\xi_L(t) + u_L^T(t)R_L u_L(t)\right\} dt, \tag{18}$$

where Q_L (> 0) and R_L (> 0) are weighting matrices, and ρ (> 0) is an adjustment parameter. This yields the state feedback control law

$$u_L(t) = K_\rho\xi_L(t),\ K_\rho = -R_L^{-1}CP_\rho, \tag{19}$$

where P_ρ is a positive symmetrical solution of the Riccati equation

$$AP_\rho + P_\rho A^T - PC^T R_L^{-1} CP_\rho + \rho Q_L = 0. \tag{20}$$

Step 3. Set the observer gain to

$$L = -K_\rho^T. \tag{21}$$

Step 4. Use (21) to calculate $G(s)$ in (11). Check if (10) holds. If it does not hold, then increase ρ until L satisfies (10).

4. Numerical Verification

This section concerns a demonstration of the validity of the EID-based method of designing an ASC system.

A model of a 10-DOF 50-m-high building was used in the simulations [22, 23]. Actuators are located on the first to the fifth DOFs. The parameters in (3) are

$$n = p = 10,\ l = 5, \tag{22}$$

$$M_S = \mathrm{diag}\{m_1, m_2, \cdots, m_{10}\}, \tag{23}$$

$$C_S = \begin{bmatrix} c_1 + c_2 & -c_2 & \cdots & 0 \\ -c_2 & c_2 + c_3 & \cdots & 0 \\ \vdots & \vdots & \ddots & \vdots \\ 0 & 0 & \cdots & c_{10} \end{bmatrix}, \tag{24}$$

$$K_S = \begin{bmatrix} k_1 + k_2 & -k_2 & \cdots & 0 \\ -k_2 & k_2 + k_3 & \cdots & 0 \\ \vdots & \vdots & \ddots & \vdots \\ 0 & 0 & \cdots & k_{10} \end{bmatrix}, \tag{25}$$

$$E_u = \begin{bmatrix} 0 & 0 & 0 & 0 & 0 & 1 & -1 & 0 & 0 & 0 \\ 0 & 0 & 0 & 0 & 0 & 0 & 1 & -1 & 0 & 0 \\ 0 & 0 & 0 & 0 & 0 & 0 & 0 & 1 & -1 & 0 \\ 0 & 0 & 0 & 0 & 0 & 0 & 0 & 0 & 1 & -1 \\ 0 & 0 & 0 & 0 & 0 & 0 & 0 & 0 & 0 & 1 \end{bmatrix}^T \tag{26}$$

$$E_g = \begin{bmatrix} 1 & 1 & 1 & 1 & 1 & 1 & 1 & 1 & 1 & 1 \end{bmatrix}^T, \tag{27}$$

$$C = \begin{bmatrix} I_{10} & 0_{10\times 10} \end{bmatrix}, \tag{28}$$

and

$$\begin{cases} m_1 = m_2 = \cdots = m_{10} = 9800\ \mathrm{kg}, \\ k_1 = 2.0809 \times 10^7\ \mathrm{N/cm},\ k_2 = 1.9653 \times 10^7\ \mathrm{N/cm}, \\ k_3 = 1.8497 \times 10^7\ \mathrm{N/cm},\ k_4 = 1.7341 \times 10^7\ \mathrm{N/cm}, \\ k_5 = 1.6184 \times 10^7\ \mathrm{N/cm},\ k_6 = 1.5028 \times 10^7\ \mathrm{N/cm}, \\ k_7 = 1.3872 \times 10^7\ \mathrm{N/cm},\ k_8 = 1.2716 \times 10^7\ \mathrm{N/cm}, \\ k_9 = 1.1560 \times 10^7\ \mathrm{N/cm},\ k_{10} = 1.0404 \times 10^7\ \mathrm{N/cm}, \\ c_i = 0.0064 \times k_i\ \mathrm{Ns/m},\ i = 1, 2, \ldots, 10. \end{cases} \tag{29}$$

The fundamental period of the building is 1.0 s, and the viscous damping ratio is 2% [24].

Note that seismic waves usually have frequencies of less than 10 Hz, which is equivalent to 62.8 rad/s. The parameters of the low-pass filter were chosen to be

$$T = 0.001 \text{ s}, \ K_F = 0.9. \tag{30}$$

The weighting matrices

$$Q_K = 10^9 \times I_{40}, \ R_K = I_5 \tag{31}$$

were used in (12) to design the optimal feedback gain, K_P.

The parameters

$$Q_L = 10^{10} \times I_{40}, \ R_L = I_{10}, \ \rho = 10^{20}, \tag{32}$$

were used in (18) to design a state observer.

To better assess the performance of the EID-based ASC system, we compared it to an SMC system, an LQR system, and no control (NC).

SMC is an advanced control method that is very effective in rejecting disturbances [25]. The sliding-mode controller is given by

$$u_f(t) = K_S \text{sign}(u_S(t)), \ u_S(t) = K_P \hat{\xi}(t), \tag{33}$$

where K_S is a positive-definite matrix. Let

$$s(t) = -K_P \xi(t), \tag{34}$$

a sliding hyperplane be

$$\Omega = \{\xi(t) : \ s(t) = 0\}, \tag{35}$$

and the Lyapunov function be

$$V(t) = \frac{1}{2} s^2(t). \tag{36}$$

The condition

$$-K_P B_u = R_K^{-1} B_u^T P B_u > 0 \tag{37}$$

guarantees a convergence subspace

$$\|\xi(t)\|_2 < \frac{\|K_P B_u (K_S - \alpha I_n)\|_2}{\|K_P A\|_2}, \tag{38}$$

which means that $dV(t)/dt < 0$ holds outside it, where α is a positive constant that is determined by the bounds on the disturbances [26, 27].

Accelerograms for the five earthquakes listed below were used to assess the performance of the various control methods:

1. 1940 El-Centro earthquake (El-Centro quake),
2. 1968 Hachinohe earthquake (Hachinohe quake),
3. 1995 Kobe earthquake (Kobe quake),
4. 1993 Noto peninsula earthquake (Noto quake), and
5. 1952 Taft earthquake (Taft quake)

Their ground accelerograms and power spectral densities (Fig. 4) are quite different from each other. The data for the Hachinohe and Noto quakes contain mainly low-frequency components; and the components of the El-Centro, Kobe, and Taft quakes distribute over a wide frequency range.

Simulations were carried out for four cases:

1. NC.
2. LQR: the system in Fig. 3 without the inclusion of the EID estimate in the control law; that is, $u(t) = u_f(t)$.
3. EID: the system in Fig. 3.
4. SMC: the control law given by (33).

The interstory-drift angles are defined to be

$$\theta_i(t) = \arctan \frac{x_i(t) - x_{i-1}(t)}{h} \approx \frac{x_i(t) - x_{i-1}(t)}{h}, \ i = 1, 2, \ldots, 10, \tag{39}$$

where $x_0 = 0$, and $h = 500$ cm is the height of each DOF. The relative velocity are defined to be

$$\Delta \dot{x}_i(t) = \frac{d[x_i(t) - x_{i-1}(t)]}{dt}, \ i = 1, 2, \ldots, 10; \tag{40}$$

and the absolute acceleration is given by

$$\ddot{x}_i(t) + \ddot{x}_g(t) = \frac{d^2 x_i(t)}{dt^2} + \ddot{x}_g(t), \ i = 1, 2, \ldots, 10. \tag{41}$$

Since $\theta_i(t)$, $\Delta \dot{x}_i(t)$, and $\ddot{x}_i(t) + \ddot{x}_g(t)$ ($i = 1, 2, \ldots, 10$) are suitable for evaluating the performance of a control method from the standpoint of the effect on the structure and the people inside, they were used as performance indexes in this study.

Simulation results (Fig. 5) show that LQR control yielded smaller interstory-drift angles, smaller relative velocity, and a smaller absolute acceleration than NC did for all five earthquake accelerograms. This shows that LQR control is effective. On the other hand, incorporating the EID estimate into the LQR control law greatly reduced the interstory-drift angles for low stories, and the relative velocity and absolute acceleration for high stories. The largest reductions were 35% for the interstory-drift angles for the Taft quake, 33% for the relative velocity for the El-Centro quake, and 47% for the absolute acceleration for the Taft quake.

The SMC method yielded smaller interstory-drift angles and smaller relative velocity than EID-based control for the El-Centro and Hachinohe quakes. However, it did not suppress the absolute acceleration; so the absolute acceleration was much larger for the SMC method than for EID-based control. For example, the absolute acceleration of the first floor for the Hachinohe quake was 2795.9 cm/s^2 for the SMC method, which is more than ten times larger than 256.90 cm/s^2 for the EID-based control. The simulation results show that the EID-based control system suppressed the three indexes (39), (40), and (41) to suitable levels.

Bode plots of the gains of the control system from $\ddot{x}_g(t)$ to $x_{10}(t)$, $G_{x_{10}\ddot{x}_g}(s)$, (Fig. 6) show the effect of plugging-in the EID estimator. LQR control reduced the gain in the frequency band up to 100 Hz; and incorporating the EID estimator made a further large reduction in the gain in the frequency band up to

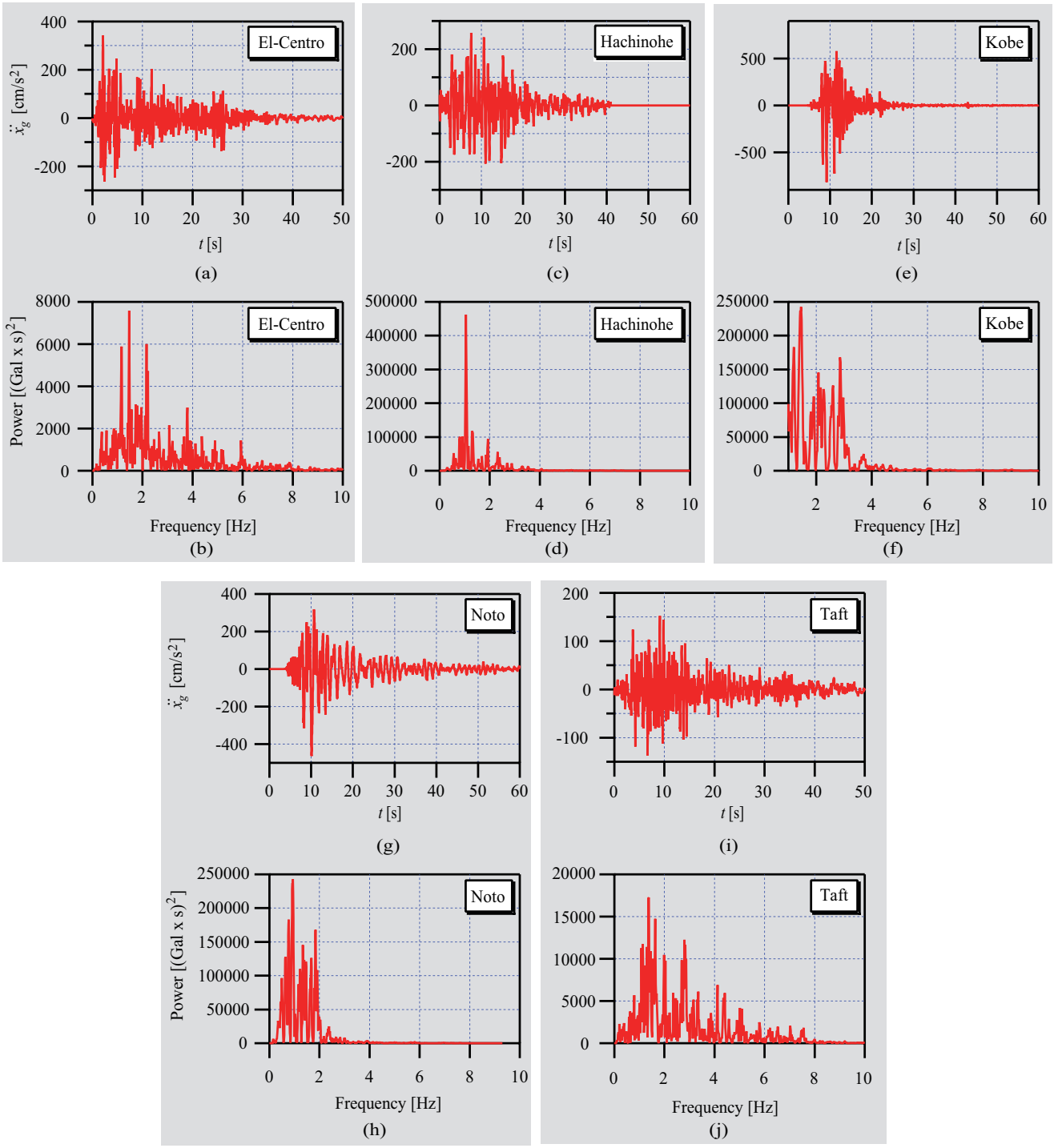

Fig. 4: Time history and power spectral density for El-Centro quake [(a) and (b)], Hachinohe quake [(c) (d)], Kobe quake [(e) and (f)], Noto quake [(g) and (h)], and Taft quake [(i) and (j)].

about 1000 Hz. More specifically, the peak gain, which occurs at a frequency of 6.28 Hz, was 119 dB smaller for LQR control than for NC, and was 430 dB smaller for EID-based control than for LQR control. This means that the vibration suppression performance at the low frequencies common in earthquakes was much better for EID-based control than for LQR control.

It is worth mentioning that using more control energy may not necessarily result in better control performance. The energy used for these three control methods is shown in Table 1. SMC used the most energy. Even though EID-based control used less energy than SMC for the Kobe quake, it yielded better results for all three indexes. And even though EID-based control used the same order of energy as LQR control did for the Kobe, Hachinohe, and Noto quakes, it showed much better

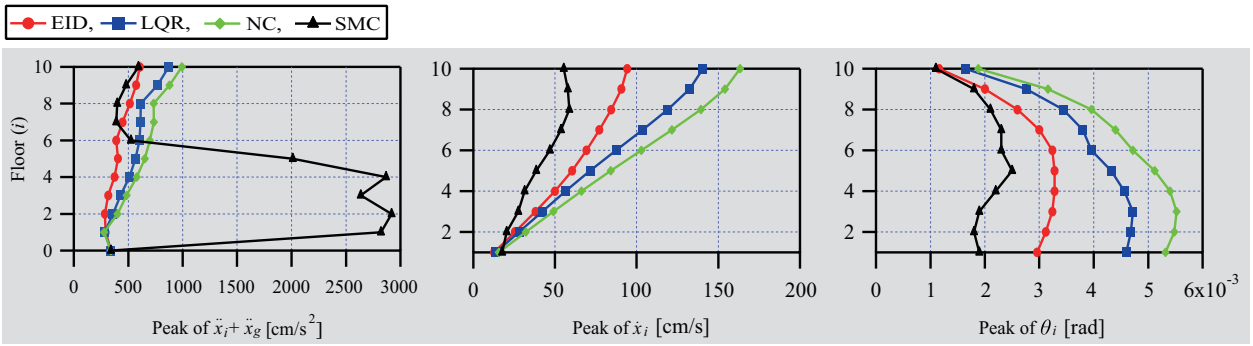

(a) Simulation results for El-Centro

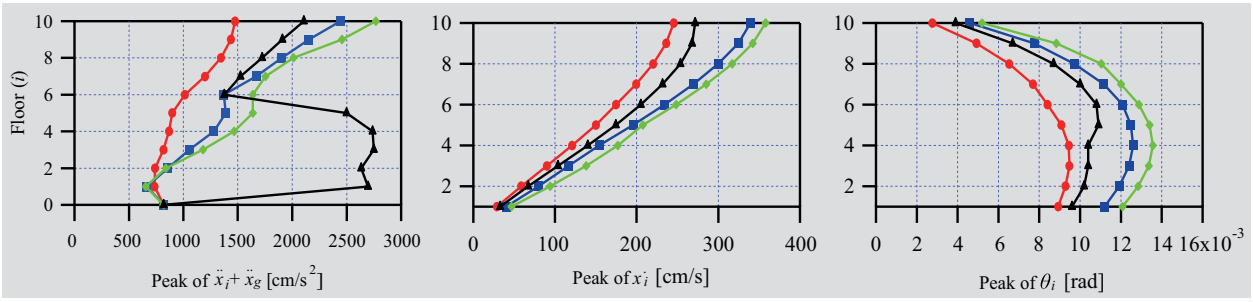

(b) Simulation results for Kobe

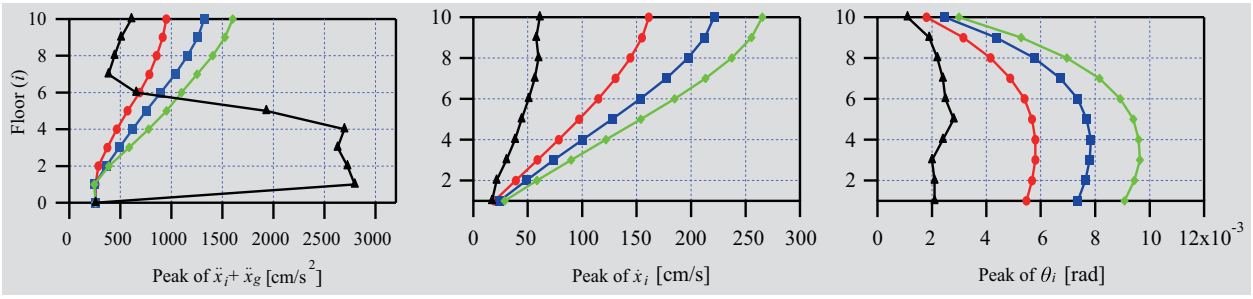

(c) Simulation results for Hachiohe

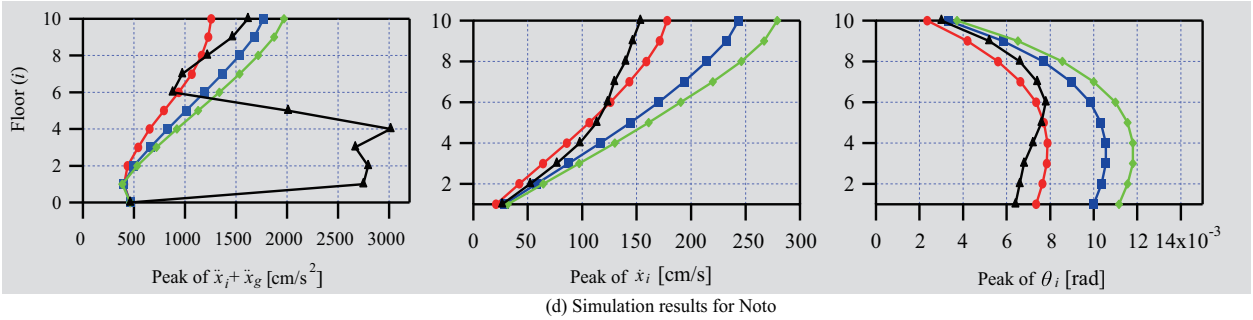

(d) Simulation results for Noto

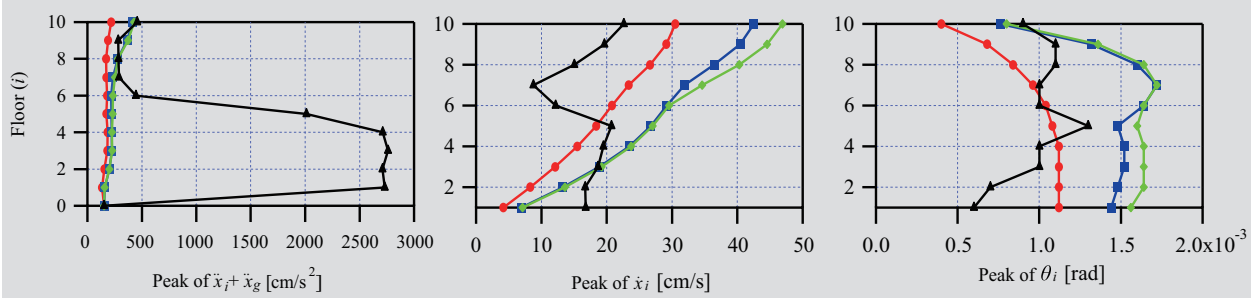

(e) Simulation results for Taft

Fig. 5: Simulation results on peak values for El-Centro quake (a), Hachinohe quake (b), Kobe quake (c), Noto quake (d), and Taft quake (e).

Table 1: Control energy ($\|u\|_2$) for LQR, SMC, and EID.

	El-Centro	Hachinohe	Kobe	Noto	Taft
LQR	3.86×10^7	3.19×10^7	3.23×10^7	1.25×10^7	6.84×10^6
SMC	3.10×10^8	3.10×10^8	3.10×10^8	3.10×10^8	3.10×10^8
EID	1.05×10^8	7.86×10^7	6.33×10^7	4.62×10^7	2.55×10^7

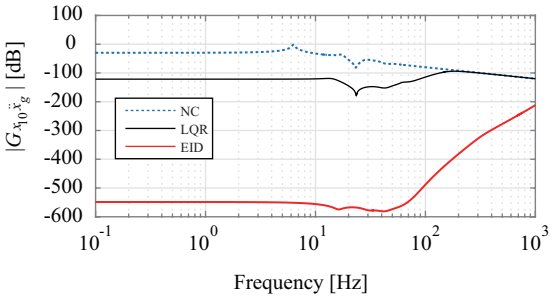

Fig. 6: Bode plots of system gain from $\ddot{x}_g(t)$ to $x_{10}(t)$ for NC, and control system in (2) without and with EID estimator.

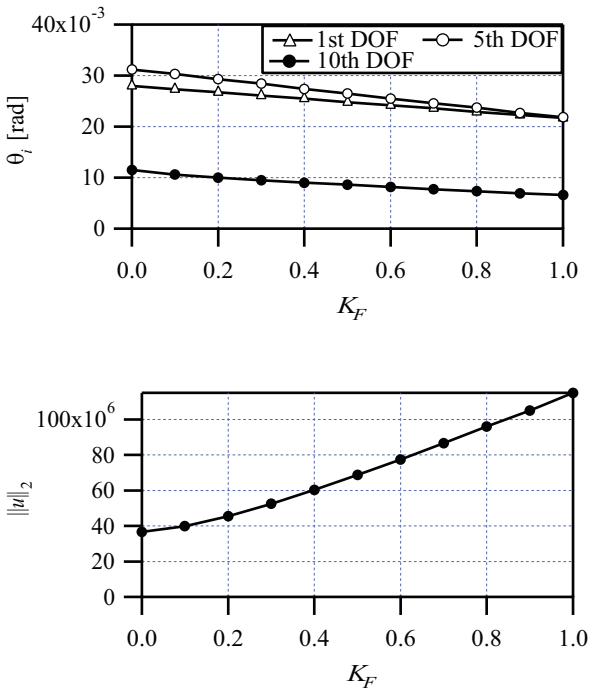

Fig. 7: Relationships between K_F and interstory-drift angles, and K_F and $\|u\|_2$ for Kobe quake.

vibration suppression performance.

EID-based control enables the trade-off between control performance and input energy to be adjusted by means of the gain of the low-pass filter, K_F. Figure 7 shows how drift and $\|u\|_2$ depend on K_F. $K_F = 0$ means LQR control, which is given by (31); and $K_F = 1$ means the best performance for EID-based control. Clearly, the adjustment of K_F provides flexibility in tuning the control performance.

5. Conclusion

In this study, the EID method was used to design an ASC system, and its validity was demonstrated using a model of a ten-DOF building. The control system has a simple structure: It can be viewed as a conventional control system (state observer + state feedback) enhanced by the plugging-in of an EID estimator. The EID estimator contains a first-order low-pass filter, which selects the angular frequency band for the estimation and suppression of vibrations. This study clarified the following points:

- Since an EID-based ASC system has two DOFs, it can provide better vibration suppression performance than a one-DOF ASC system can, provided that it is well designed.
- A comparison with LQR control and SMC using data on the 1940 El-Centro, 1968 Hachinohe, 1995 Kobe, 1993 Noto Peninsula, and 1952 Taft earthquakes demonstrated the superiority of EID-based ASC.
- There is a trade-off between control performance and input energy, and adjustments can be made by means of the gain of the low-pass filter, K_F, in the EID estimator.
- EID-based ASC suppresses not only the interstory-drift angle, but also the relative velocity and acceleration of each DOF. This reduces both structural damage and the impact on humans.

This method can be used directly to deal with vibrations caused by high winds.

It is important and useful to examine the robustness of the EID-based ASC system and provide an upper bound for control performance. Methods of analyzing pulse-like accelerograms, for example, [28, 29], may provide us a useful tool for system evaluation. These will be the focus of future work. Another issue is the time delay in an actuator, as pointed out in [30, 31]. Since a time delay may degrade control performance, this issue will also be considered in the future.

References

[1] Spencer B. F. Jr. and Nagarajaiah S., State of the Art of Structural Control, *Journal of Structural Engineering*, 2003; 129 (7): 845-856.

[2] Korkmaz S., A review of active structural control: challenges for engineering informatics, *Computers and Structures*, 2011; 89 (23-24): 2113-2132.

[3] Ebrahimnejad M., Davoodi M., and Vaseghi-Amiri J., Active vibration control of smart building frames by feedback controllers, *Cmp. Meth. Civil Eng.*, 2010; 1 (1): 73-83.

[4] Yanik Arcan, Aldemir Unal, Bakioglu Mehmet, A new active control performance index for vibration control of three-dimensional structures,*Engineering Structures*, 2014; 62-63: 53-64

[5] Thenozhi S.an Yu W., Stability analysis of active vibration control of building structures using PD/PID control, *Engineering Structures*, 2014; 81: 208-218.

[6] Park K.-S., Kon H. M., and Ok S.-Y., Active control of earthquake excited structures using fuzzy supervisory technique, *Advances in Engineering Software*, 2002; 33 (11-12): 761-768.
[7] Cho H. C., Fadali M. S., Saiidi M. S., and Lee K. S., Neural Network Active Control of Structures with Earthquake Excitation, *Int. J. Control, Automation, and Systems*, 2005; 3 (2): 202-210.
[8] Ma Y. Q.and Qiu H.-X., Integrated Multiobjective Optimal Design for Active Control System Based on Genetic Algorithm, *Mathematical Problems in Engineering*, 2014; 2014: ID748237/1-9.
[9] Rao A. R. M. and Sivasubramanian K., Multi-objective optimal design of fuzzy logic controller using a self configurable swarm intelligence algorithm, *Computers and Structures*, 2008; 86: 2141-2154.
[10] Artard T.L. and Wharton C.R., Optimal control parameterization for displacement and acceleration demands, and local post-yield constitutive responses, *Engineering Structures*, 2012; 36: 123-133.
[11] Tovar A., Khandelwal K., Topology optimization for minimum compliance using a control strategy, *Engineering Structures*, 2013; 48: 674-682.
[12] Mei G., Kareem A., and Kantor J. C., Model Predictive Control of Structures under Earthquakes using Acceleration Feedback, *J. Engineering Mechanics*, 2002; 128 (5): 574-585.
[13] Guclu R., Sliding mode and PID control of a structural system against earthquake, *Mathematical and Computer Modelling*, 2006; 44 (1-2): 210-217.
[14] Wang S. G., Robust active control for uncertain structural systems with acceleration sensors, *J. Struc. Control*, 2003; 10: 59-76.
[15] Mechbal N. and Nóbrega E. G. O., Spatial H_∞ approach to damage-tolerant active control, *Struc. Control Health Monit.*, 2015; 22 (8): 1148-1172.
[16] Du H., Zhang N., Samali B., and Naghdy F., Robust sampled-data control of structures subject to parameter uncertainties and actuator saturation, *Engineering Structures*, 2012; 36: 39-48.
[17] Oveisi A., Shakeri R., Robust reliable control in vibration suppression of sandwich circular plates, *Engineering Structures*, 2016; 116: 1-11.
[18] Horowitz I. M., *Synthesis of Feedback Systems*, Academic Press, 1963.
[19] She J., Fang M., Ohyama Y., Hashimoto H., and Wu M., Improving Disturbance Rejection Performance Based on an Equivalent-Input-Disturbance Approach, *IEEE Trans. Industrial Electronics*, 2008; 55 (1): 380-389.
[20] She J., Xin X., and Pan Y., Equivalent-Input-Disturbance Approach – Analysis and Application to Disturbance Rejection in Dual-Stage Feed Drive Control System, *IEEE/ASME Trans. Mechatronics*, 2011; 16 (2): 330-340.
[21] She J., Sekiya K., Wu M., and Lei Q., Active Structural Control with Input Dead Zone Based on Equivalent-Input-Disturbance Approach, *Proc. of 36th Annual Conference on IEEE Industrial Electronics Society (IECON 2010)*, 2010; 47-52.
[22] Kitamura H., Zaitsu K., Mayahara T., Energy balance-based seismic response prediction method for response controlled buildings using hysteresis dampers, *Journal of structural and construction engineering*, 2006; 599: 71-78.
[23] Sato D., Kitamura H., Sato D., Sato T., Yamaguchi M., Wakita N., Watanuki Y., Energy balance-based seismic response prediction method for response control structures with hysteresis dampers and viscous dampers, *Journal of structural and construction engineering*, 2014; 79(699): 631-640.
[24] Willford M., Whittaker A., and Klemencic R., *Recommendations for the Seismic Design of High-Rise Buildings*, Council on Tall Buildings and Urban Habitat (CTBUH), Chicago, 2008.
[25] Edwards C., Colet E. F., and Fridman L., *Advances in Variable Structure and Sliding Mode Control (Lecture Notes in Control and Information Sciences)*, Springer-Verlag Berlin, 2006.
[26] Choi H. H., On the existence of linear sliding surfaces for a class of uncertain dynamic systems with mismatched uncertainties, *Automatica*, 1991; 35: 1707-1715.
[27] She J., Pan Y., Hashimoto H., Lei Q., and Wu M., Equivalent-Input-Disturbance Approach Enables Sliding-Mode Control Systems to Reject Unmatched Disturbances, *Proc. the 2015 IEEE International Conference on Industrial Technology (ICIT 2015)*, 2015; 226-231.
[28] Baker J. W., Quantitative Classification of Near-Fault Ground Motions Using Wavelet Analysis, *Bulletin of the Seismological Society of America*, 2007; 97 (5): 1486-1501.
[29] Zhai C., Chang Z., Li S., Chen Z., Xie L., Quantitative Identification of Near-Fault Pulse-Like Ground Motions Based on Energy, *Bulletin of the Seismological Society of America*, 2013; 103 (5): 2591-2603.
[30] López-Almansa F. and Rodellar J., Control Systems of Building Structures by Active Cables, *J. Struct. Eng.*, 1989; 115 (11): 2897-2913.
[31] López-Almansa F. and Rodellar J., Feasibility and robustness of predictive control of building structures by active cables, *Earthquake Engineering and Structural Dynamics*, 1990; 19: 157-171.